Research Square

Preprints are preliminary reports that have not undergone peer review.
They should not be considered conclusive, used to inform clinical practice,
or referenced by the media as validated information.

PI3K/AKT Pathway Promotes Keloid Fibroblasts Proliferation by Enhancing Glycolysis Under Hypoxia

Qifei Wang
Peking University Third Hospital
Xin Yang
Peking University Third Hospital
Jianxun Ma
Peking University Third Hospital
Xiang Xie
Peking University Third Hospital
Yimou Sun
Peking University Third Hospital
Xu Chang
Peking University Third Hospital
Hongsen Bi
Peking University Third Hospital
Hongyu Xue
Peking University Third Hospital
Zelian Qin (qinzl@bjmu.edu.cn)
Peking University Third Hospital https://orcid.org/0000-0003-1420-4576

Research

Keywords: keloid, fibroblast, PI3K/AKT pathway, glucose metabolism, glycolysis, function

Posted Date: November 2nd, 2021

DOI: https://doi.org/10.21203/rs.3.rs-1022613/v1

License: This work is licensed under a Creative Commons Attribution 4.0 International License.
Read Full License

Abstract

Background

Keloids are disfiguring fibro-proliferative disorders characterized by glucose metabolism reprogramming, namely elevated glycolysis and compromised oxidative phosphorylation. Our previous study demonstrated altered glucose metabolism and enhanced phosphorylation of the PI3K/AKT pathway in keloid fibroblasts (KFb) under hypoxic conditions. However, whether the PI3K/AKT pathway influences KFb cell function by regulating glucose metabolism under hypoxic conditions remains unclear.

Results

Our findings revealed that when the PI3K/AKT pathway was inactivated with LY294002 under hypoxia, the protein expression of glycolytic enzymes GLUT1, HK2, PFKFB3, PGK1, ENO1, PKM2, and LDHA decreased under hypoxia, while the amount of mitochondria and mitochondrial membrane potential (MMP) increased, and mitochondrial ultrastructure in KFb remained unchanged. The key parameters of extracellular acidification rate (ECAR) markedly diminished, and those of oxygen consumption rate (OCR) significantly increased after inhibition of the PI3K/AKT pathway. When the PI3K/AKT pathway was suppressed, the levels of ROS and mitochondrial ROS were significantly increased. Meanwhile, cell proliferation, migration, and invasion were inhibited, and apoptosis was increased when the PI3K/AKT pathway was blocked. Additionally, cell proliferation was compromised when KFb were treated with both SC79 (an activator of the PI3K/AKT pathway) and 2-DG (an inhibitor of glycolysis), compared to the SC79 group. Moreover, a positive feedback mechanism was demonstrated in the PI3K/AKT pathway and HIF-1α.

Conclusions

Our data collectively demonstrated that the PI3K/AKT pathway promotes proliferation and inhibits apoptosis in KFb under hypoxia by regulating glycolysis, indicating that the PI3K/AKT signaling pathway could be a therapeutic target for keloids.

Background

Keloids are pathological scars characterized by uncontrolled proliferation of dermal fibroblasts and excessive deposition of extracellular matrix (ECM) [1]. As a result of abnormal wound healing, keloids are clinically accompanied by itching, pain, cosmetic deformities, and joint dysfunction [2]. Additionally, keloids exhibit cancer-like properties, including outgrowth beyond the boundary of the initial wound and invasion into adjacent normal skin [3]. Clinically, multiple approaches, including surgical removal combined with steroid injections, laser therapy, radiotherapy, and compression therapy are available for the prevention and treatment of keloids [4]. However, the above therapeutic approaches are

unsatisfactory and cannot prevent recurrence. In recent decades, genetics, inflammation, tumor-related factors, and immune cells have been shown to participate in the pathogenesis of keloids [5–8]. However, the mechanisms of keloid pathogenesis are poorly documented, and keloid scarring continues to be one of the most challenging skin problems.

Metabolic reprogramming is an emerging hallmark of cancer. Altered glucose metabolism generally occurs in the form of the Warburg effect (aerobic glycolysis), which was first observed in cancer cells. It describes a phenomenon that occurs even in an oxygen-enriched environment. Cancer cells are dependent on glycolysis to rapidly generate ATP from glucose. It has been demonstrated that aerobic glycolysis facilitates the autonomous proliferation and survival of cancer cells by providing substrates for macromolecule synthesis, apoptosis regulation, and redox homeostasis. Furthermore, it has been established that the Warburg effect exists in various cells and disorders, including immune cells [7], stem cells [9], sepsis [10] and Alzheimer's disease [11]. Interestingly, altered metabolism was also observed in keloids. Our previous studies revealed that KFb exhibited elevated glucose intake and lactate accumulation, enhanced mRNA and protein expression of glycolytic enzymes, and attenuated mitochondrial oxidative phosphorylation. Additionally, an increase in the ECAR (indicating glycolytic level) and a decrease in OCR (indicating mitochondrial respiration) have been reported.

Tissue hypoxia exists in various solid tumors and is clinically related to resistance to therapy andpoor prognosis. The hypoxic microenvironment in keloids results from massive collagen deposition and partially or completely occluded capillaries. Okuno et al. [12] reported that the keloid center was a hypoxic zone and exhibited higher expression of hypoxia inducible factor-1α (HIF-1α) when compared with the margin zone. The hypoxic microenvironment in keloids facilitates epithelial-mesenchymal transition (EMT) [13] and modulates apoptosis [14]. Additionally, our previous studies indicated that hypoxia significantly promoted KFb proliferation, migration, invasion, and collagen synthesis [15]. Furthermore, insufficient oxygen supply in keloids profoundly alters glucose metabolism in KFb. Our previous work demonstrated enhanced glycolysis and compromised mitochondrial respiration in KFb under hypoxic conditions [15]. Moreover, hypoxia promotes the activation of metabolic pathways, including HIF-1α [16] and the PI3K/AKT signaling pathway [17].

The PI3K/AKT pathway is a major growth regulatory pathway in mammalian cells and is frequently dysregulated in human cancers [18]. The pathway plays a major role in critical physiological functions and multiple cellular processes, including survival, growth, and proliferation [19]. Additionally, this signaling pathway promotes the reprogramming of glucose metabolism [20, 21]. The stimulation of diverse oncogenes and growth factor receptors triggers PI3K activation, which has diverse downstream effects on mammalian target of rapamycin complex 1 (mTORC1), members of the forkhead box O (FOXO) family of transcription factors, and glycogen synthase kinase 3 (GSK3). Activated PI3K can phosphorylate phosphatidylinositol- 4,5-bisphosphate (PIP2) to generate phosphatidylinositol- 3,4,5-trisphosphate (PIP3), and the process can be inversed by phosphatase and tensin homolog deleted on chromosome ten (PTEN). PIP3 leads to AKT phosphorylation by activating pyruvate dehydrogenase kinase 1 (PDK1).These downstream effectors play a key role in cellular metabolic reprogramming [22,

23]. Additionally, AKT phosphorylation directly regulates the phosphorylation and activation of specific glycolytic enzymes, including hexokinase 2 (HK2) and phosphofructokinase 1 (PFK1). In addition to the direct regulation of glycolytic enzymes, the PI3K-AKT signaling pathway also drives aerobic glycolysis through increased protein expression of glucose transporters and glycolytic enzymes modulated through the regulation of downstream transcription factors, including HIF-1α and MYC [24–26]. Accumulating evidence demonstrates that the PI3K-AKT signaling pathway plays a critical role in facilitating glucose intake and glycolysis under physiological conditions and in the context of the tumor microenvironment. However, further studies are required to determine whether the activation of PI3K/AKT signaling enhances mitochondrial respiration.

While accumulating studies have demonstrated the key role of the PI3K-AKT pathway in the regulation of glucose metabolism in a range of cancer cells, the mechanism of PI3K-AKT signaling in KFb is not clear. Keloids manifest some similar biological features as solid tumors, including metabolic reprogramming, and our previous study showed upregulated phosphorylation of the PI3K-AKT pathway in KFb. Herein, we postulated that the PI3K-AKT pathway modulates glucose metabolism, which further influences cell function in keloid fibroblasts under hypoxic conditions. In the present study, we investigated the effects of the PI3K-AKT pathway on glycolysis and mitochondrial functions, and the subsequent role of glycolysis in regulating cell functions in KFb under hypoxia. In addition, the interactions between the PI3K/AKT pathway and HIF-1α under hypoxia were also explored.

Materials And Methods

Isolation and culture of fibroblasts

The study was approved by the Ethics Committee of the Peking University Third Hospital (IRB00006761-2014173). The study was conducted in accordance with the Declaration of Helsinki. Written informed consent was obtained from all participants. Keloids were diagnosed based on clinical and histological evidence, and keloid samples were obtained from subjects who underwent surgical procedures. None of the participants received treatment for keloids before surgical removal. Basic information of the keloid specimens is described in Supplementary Table S1. Fibroblast extraction and culture were performed as described previously with slight modifications [15]. Briefly, primary keloid fibroblasts were extracted using the collagenase digestion method and were cultured in Dulbecco's modified Eagle's medium (DMEM) (HyClone, USA), with 10% fetal bovine serum (FBS) (Gibco, USA) and 1% penicillin/streptomycin (HyClone, USA), in an incubator conditioned at 37°C and 5% CO_2. Four to six passages of fibroblasts were used in the experiments.

LY 294002 concentration determination and proliferation assays

To determine the optimal LY294002 concentration that inhibited cell proliferation, KFb was cultured in DMEM containing a series of LY294002 doses (0, 1, 5, 10, 25, and 50 μM). Briefly, 1.5×10^5 cells were

seeded into six-well culture plates and cultured in different concentrations of LY294002 under hypoxia (3%) or normoxia for 48 h. KFb were harvested, and the total number was calculated based on cell counting under a microscope (Leica, Germany). Additionally, we investigated the effect of PI3K inhibition on KFb proliferation at different time points. We cultured 1.5×10^5 cells in six-well plates containing different doses of LY294002 (0, 5, and 25 μM) and KFb were incubated for 24, 48, 72, and 96 h under hypoxia or normoxia. Cells were collected and counted by cell counting. Finally, to investigate whether glycolysis is involved in the regulation of PI3K activation and proliferation, 1.5×10^5 KFb seeded into six-well culture plates were treated with phosphate-buffered saline (PBS), LY294002 (25 μM), SC79 (10 μM) or SC79 (10 μM) combined with 2-deoxy-d-glucose (2-DG, 2 mM), respectively. Following which, KFb was incubated for 24, 48, 72, and 96 h under hypoxia or normoxia. Cells were harvested and the total number was calculated as described above.

Migration and invasion assays

The inhibition of LY294002 on KFb migration was assessed by transwell chambers with 8.0 μM pores (Corning, USA). Briefly, 2×10^5 KFb were seeded into 6 cm cell culture plates with complete medium containing different doses of LY294002 (0, 5, and 25 μM) and were incubated for 24 h under hypoxia or normoxia. Cells were collected and the cell concentration was adjusted to 5×10^5 ml with DMEM containing 0, 5, and 25 μM of LY294002. KFb (1×10^4) were seeded into the upper compartment with 200 μl DMEM, and 500 μl complete medium containing 10% FBS was added to the lower compartment. KFb cells were cultured with previous oxygen levels for another 24 h. The upper cells were removed using a cotton swab. The migrated cells were fixed with 4% paraformaldehyde for 20 min and stained with 0.1% crystal violet for 20 min. The number of migrated cells was counted in five random fields under a microscope (100 × magnification).

In our study, the invasion experiment differed slightly from the migration assay. Matrigel was diluted in DMEM to a volume ratio of 1:8. diluted matrigel (40 μl) was added to the upper compartment and the transwell chambers were incubated for 2 h. Cells (2×10^4) that had been treated with LY294002 (0, 5, and 25 μM) under hypoxia or normoxia were seeded into the upper compartment of the chamber and were cultured in incubators with the previous oxygen environment for 36 h. The other steps were the same as those used in the migration assays.

Apoptosis assay

The apoptotic level of KFb was determined with an Annexin V-PE/7-AAD apoptosis detection kit (KeyGEN, China) using flow cytometry, according to the manufacturer's instructions. In brief, KFb were seeded into six-well plates at a density of 2×10^5 cells/well and treated with diverse LY294002 levels (0, 5, and 25 μM) under hypoxia or normoxia for 24 h. KFb were collected with 0.25% trypsin not containing EDTA and resuspended in 50 μl binding buffer and 5 μl 7-AAD. The cells were incubated for 20 min in the dark. Then, 450 μl binding buffer and 1 μl Annexin V-PE were added to the above solution and incubated for 20 min in the dark. Flow cytometry (BD, USA) was used to analyze the effect of PI3K inhibition on KFb apoptosis.

Western blotting

Western blotting analysis was performed as described in our previous study [15]. Total proteins were extracted using RIPA lysis buffer (Solarbio, China) combined with phosphatase (1:100) and protease (1:50) inhibitor cocktail (Solarbio, China). The cell lysates were centrifuged at 12,000 rpm/min at 4°C for 10 min. Protein concentrations were estimated using a bicinchoninic acid (BCA) protein assay kit (Pulilai, China). Protein samples (30 μg) were separated by 10% sodium dodecyl sulfatepolyacrylamide gel electrophoresis (SDS-PAGE) at 80 V for 20 min and then 120 V for 1 h, and were transferred to polyvinylidene difluoride (PVDF) membranes with 0.45 μm of pores (Millipore, MA, USA) at 220 mA for 60 min. PVDF membranes were repeatedly washed using tris-buffered saline (TBS) containing Tween 20 (TBST) and blocked with 5% bull serum albumin (BSA) blocking buffer at room temperature for 1 h. Then, the PVDF membranes were incubated overnight at 4°C with primary antibodies (Supplementary Table S2). The PVDF membranes were then washed and incubated with HRP-conjugated secondary antibody and washed with TBST (0.1%). Finally, the signals were visualized using an enhanced chemiluminescence system (Amersham Pharmacia Biotech, United Kingdom). Densitometric analysis was performed using ImageJ software.

Reactive oxygen species (ROS) and mitochondrial ROS determinations

ROS and mitochondrial ROS (mitoROS) levels were measured using a Reactive Oxygen Species Assay Kit (Beyotime, China) and MitoSOX Red reagent (Invitrogen, USA), respectively, according to the manufacturer's instructions. Briefly, 2×10^5 KFb were seeded into 6-well plates and cultured in complete culture medium containing different concentrations of LY294002 (0, 5, and 25 μM) in incubators under hypoxia or normoxia at 37°C for 24 h. For ROS detection, KFb were harvested with 0.25% trypsin and incubated with 10 μM DCFH-DA working solution for 20 min at 37°C in the dark. For mitoROS investigation, cells were incubated in 1 ml of 5 μM MitoSOX reagent working solution at 37°C in the dark. The cells were then washed twice with DMEM without FBS to remove the working solution that did not enter the cells. Finally, the fluorescence intensity was assessed using a flow cytometer (BD, USA).

Mitochondrial mass and MMP measurements

Mitochondrial mass and MMP were measured using Mito-Tracker Green (Beyotime, China) and JC-1 (Beyotime, China), respectively. Briefly, 2×10^5 cells were seeded into 6-well plates and incubated with complete culture medium containing different concentrations of LY294002 (0, 5, and 25 μM) in incubators under hypoxia or normoxia at 37°C for 48 h for mitochondrial mass determination or for 24 h for MMP measurement. To measure mitochondrial mass, cells were stained with 200 nM prewarmed MitoTracker Green staining solution (Beyotime, China) at 37°C in the dark for 15 min. For MMP assessment, cells were incubated with 500 μl 10 μg/ml JC-1 (Beyotime, China) for 20 min at room temperature in the dark. Finally, the cells were resuspended in 500 μl DMEM without serum. Fluorescence intensities were analyzed using a flow cytometer (BD Biosciences). Green fluorescence intensity was

recorded for mitochondrial mass analysis, and the ratio of red and green fluorescence intensities was documented for MMP comparison.

Analyzing ECAR and OCR

The XF96 Extracellular Flux Analyzer (Seahorse Bioscience, USA) was used to evaluate glycolysis and mitochondrial oxidative phosphorylation using ECAR and OCR, respectively. Briefly, 6×10^5 KFb were seeded into 10 cm cell culture plates and cultured in complete culture medium containing 25 μM LY294002, 10 μM SC79, or 2 mM 2-DG in incubators under hypoxia or normoxia at 37°C for 24 h. Cells were collected with 0.25% trypsin, and 1×10^4 cells/well were resuspended in the previous medium conditions, seeded into a special 96-well plate, and were incubated under previous oxygen conditions for 24 h. Calibration solutions were added into each well of the probe plates and placed in a humidified incubator without CO_2 overnight. The Seahorse XF stress test assay medium was prepared in accordance with the protocol for glycolysis and mitochondrial stress tests. The cells were washed twice with the conditioned medium, and the final volume in each well was 175 μl before the Seahorse assay. For ECAR determination, cells were treated with sequential injections of glucose (10 mM), oligomycin (2 μM), and 2-DG (50 mM). While for OCR measurement, oligomycin (2 μM), FCCP (2 μM), and rotenone/antimycin A (1 μM) were loaded sequentially. The results were normalized to the total protein content measured by a BCA assay. ECAR and OCR are reported in mpH/min/prot and pmol/min/ug prot, respectively.

Mitochondrial ultrastructure observation

Transmission electron microscopy was performed to observe mitochondrial ultrastructure. After treatment with LY294002 (0 and 25 μM) for 48 h, cells were harvested and fixed with 2.5% glutaraldehyde and then fixed in 1% osmium tetroxide at 4°C for 2 h. Cell clumps were dehydrated in a series of ethanol gradients, embedded in epoxy resin, polymerized at 60°C, cut into 50 nm sections, and stained with 3% uranyl acetate and lead citrate. Six random fields in each sample were chosen and observed under a transmission electron microscope (TEM) (JEM1400 Plus, Japan).

Statistical analysis

All data are presented as mean ± standard deviation of at least three independent experiments. GraphPad Prism 7.0 (GraphPad Prism Software, USA) was used for statistical analysis. Normal distribution and homogeneity of variance were assessed using the Kolmogorov-Smirnov and Levene tests, respectively. Comparisons between the two groups were performed with Student's t-test, and comparisons of multiple groups were carried out by one-way or two-way ANOVA combined with a Bonferroni multiple comparison post-test. Statistical significance was set at $p < 0.05$.

Results

Inactivation of the PI3K-AKT pathway inhibited glycolysis

The PI3K/AKT pathway plays a central role in cell growth, proliferation, survival, and glucose metabolism. Our previous studies demonstrated altered glucose metabolism and enhanced phosphorylation of PI3K and AKT in KFb under hypoxia. However, regulation of the PI3K-AKT signaling network in glucose metabolism in KFb under hypoxic conditions has not been investigated. Hypoxia concentration was optimized in our previous work and 3% hypoxia was used in experiments. In this study, to determine the dose of PI3K inhibitor LY294002 in the following experiments, cell viabilities of KFb treated with different concentrations of LY294002 under 3% hypoxia were observed. The results suggested that inactivation of the PI3K-AKT pathway with LY294002 reduced KFb viability in a concentration-dependent manner, with inhibition using a 25 μM concentration being obvious, and the inhibitory effect did not change markedly with an increase in concentration (Figure 1A). Therefore, the doses of LY294002 in the follow-up experiments were 0 μM, 5 μM, and 25 μM.

Elevated phosphorylation of the PI3K-AKT signaling pathway altered glucose metabolism by promoting glucose intake and the expression of glycolytic enzymes. In the present study, we investigated the protein expression of glycolytic enzymes, including GLUT1, HK2, PFKFB3, PGK1, ENO1, PKM2, and LDHA in KFbs treated with or without 25 μM LY294002 for 24 h under hypoxia or normoxia. Interestingly, HK2, PFKFB3 and LDHA protein levels were profoundly attenuated by LY294002 under normoxia (Fig. 1. D, E and I). Importantly, the inhibition of the PI3K-AKT signaling pathway downregulated the protein levels of glycolytic enzymes under hypoxia (Fig. 1. B-I).

PI3K inhibition altered mitochondrial mass, MMP, and ultrastructure

The PI3K-AKT pathway is indispensable for sustaining mitochondrial functions and healthy conditions. Although the role of PI3K-AKT signaling in mitochondrial functions has been extensively studied, it remains unclear whether PI3K inhibition promotes or inhibits mitochondrial respiration in KFb under hypoxia. In the present study, we observed mitochondrial mass, MMP, and ultrastructure when KFb was treated with a PI3K inhibitor. KFb cells were treated with LY294002 (0, 5, and 25 μM) for 48 h under hypoxia or normoxia. Results detected by flow cytometry with a mitochondrial green explorer showed that the inhibition of the PI3K-AKT pathway increased mitochondrial mass in a dose-dependent manner, and its enhancement was more significant under hypoxia (Fig. 2. A-B). MMP reflects healthy mitochondrial conditions, and decreased MMP indicates that cells are in an early stage of apoptosis. Flow cytometry analysis combined with JC-1 revealed hyperpolarization of MMP after PI3K inhibition for 24 h (Fig. 2. C-D). Mitochondrial morphological structure is closely linked to its biological functions. Hence, we observed mitochondrial ultrastructure using transmission electron microscopy (TEM). After treatment with LY294002 for 48 h under hypoxia or normoxia, mitochondrial ultrastructure in KFb appeared similar to previous conditions, manifesting swollen mitochondria, cristae effacement, and vacuolization (Fig. 2E).

PI3K suppression reduced the ECAR and increased the OCR

The PI3K-AKT signaling network plays a complex role in modulating glycolysis and mitochondrial functions. To directly monitor the glucose metabolism in KFb after PI3K inhibition, the Seahorse XF instrument was explored in this study. ECAR reflects glycolysis. A glycolysis stress test was performed to determine the glycolytic level. The results suggested decreased key parameters of glycolytic flux, including non-glycolytic acidification, glycolysis, glycolytic capacity, and glycolytic reserve in KFb treated with PI3K inhibitor for 24 h both under hypoxia and normoxia (Fig. 3. A-E). Furthermore, KFb under hypoxia exhibited lower ECAR than that under normoxia when cells were treated with LY294002. OCR represents mitochondrial respiration; we also performed a Mito Stress Test to evaluate mitochondrial respiration. After treatment with PI3K inhibitors, KFb showed an increase in key parameters including non-mitochondrial respiration, basal respiration, maximal respiration, spare capacity, and ATP production under both hypoxic and normoxic conditions (Fig. 3. F-M). KFb are more sensitive to LY294002 under hypoxic conditions. Moreover, the ratio of OCR/ECAR increased remarkably in KFb after PI3K inactivation, indicating a metabolic shift to oxidative phosphorylation.

Blockade of the PI3K-AKT signaling pathway suppresses proliferation, migration, and invasion, and elevates apoptosis

The PI3K-AKT pathway is crucial for biological functions, including growth, survival, and proliferation in mammalian cells and is aberrantly activated in cancer cells. Our results suggest altered glucose metabolism in KFbs treated with PI3K inhibition. However, the role of the PI3K-AKT pathway in KFb proliferation, migration, invasion, and apoptosis is yet to be investigated. In this study, KFb cells were treated with different concentrations of LY294002 and cultured under hypoxia or normoxia for 24, 48, and 72 h. The proliferation of KFb treated with LY294002 was inhibited in a dose- and time-dependent manner (Fig. 4. A-B). Furthermore, inhibition of proliferation under hypoxic conditions was more obvious than that under normoxia. In addition, the PI3K-AKT signaling network is involved in mitochondrial apoptosis. Hence, the apoptotic levels of KFb treated with the PI3K inhibitor were determined under hypoxia and normoxia. Interestingly, we observed increased apoptosis in KFb. Moreover, the pro-apoptotic effect was more distinct under hypoxic conditions (Fig. 4. C-D). The PI3K-AKT pathway is intimately linked to invasion by regulating the protein levels of MMP-2 and MMP-9. In this study, we detected the migration and invasion of KFb after the inhibition of PI3K. The migration (Fig. 4. E-F) and invasion (Fig. 4. G-H) of KFb seeded in the Transwell chamber were suppressed when the PI3K-AKT signaling pathway was inactivated.

The PI3K-AKT pathway promoted proliferation by regulating glycolysis

These results collectively indicate that the PI3K-AKT pathway regulates glucose metabolism and cell function. However, it is yet to be clarified whether glycolysis is involved in cell function modulation by the PI3K-AKT pathway. KFb was administered with PBS, LY294002, SC79 (AKT activator), and SC79

combined with 2-DG (glycolysis inhibitor). The glycolysis stress test showed lower ECAR in the LY294002 group and higher key glycolysis parameters in the SC79 group (Fig. 5. A-F). Interestingly, KFb treated with SC79 combined with 2-DG exhibited significantly lower ECAR parameters than the control group (Fig. 5. A-F). These findings indicate that glycolysis is partly regulated by the PI3K-AKT pathway. Energy generation in mammalian cells largely depend on mitochondrial oxidative phosphorylation and glycolysis. When glycolysis is markedly inhibited, cells resort to mitochondrial respiration for ATP provision. Interestingly, we observed that KFb showed attenuated OCR when the PI3K-AKT pathway was activated by SC79 (Fig. 5. G-M). Importantly, KFb treated with SC79 coupled with 2-DG exhibited higher key OCR parameters. Finally, we investigated the potential mechanism underlying the regulation of PI3K activation during proliferation. Cell proliferation was inhibited or promoted when KFb were cultured with LY294002 or SC79 (Fig. 5. N-O). This observation suggests that the PI3K-AKT pathway promotes KFb proliferation. Additionally, the rate of proliferation of KFb treated with SC79 and 2-DG was remarkably inhibited compared to that in the SC79 group (Fig. 5. N-O). These results collectively indicate that the PI3K-AKT pathway promotes proliferation by enhancing glycolysis.

The PI3K-AKT signaling network was involved in redox homeostasis

Cellular redox homeostasis is highly dependent on the balance between ROS production and elimination and is closely related to glucose metabolism. A wide range of evidence suggests that increased ROS levels in mammalian cells result in PI3K activation. However, few studies have focused on the role of the PI3K-AKT pathway in ROS generation. To observe the effect of PI3K signaling on ROS homeostasis, we determined the total ROS and mitochondrial ROS levels after KFb were treated with LY294002 under hypoxic or normoxic conditions. The results showed elevated total ROS (Fig. 6. A-B) and mitoROS (Fig. 6. C-D) levels after PI3K inhibition. Additionally, the promotion of ROS generation by PI3K inactivation under hypoxia was more obvious than that under normoxia. These findings robustly suggest that the PI3K-AKT pathway is crucial for maintaining redox homeostasis.

The PI3K-AKT pathway interacted with HIF-1α through a positive feedback mechanism

The PI3K-AKT signaling network and HIF-1α are two principal pathways for the modulation of glucose metabolism under hypoxia. However, the relationship between the two pathways in KFb remains to be elucidated. Recent studies have revealed that the activation of the PI3K-AKT pathway leads to HIF-1α accumulation in mammalian cells under hypoxic conditions. However, the effect of HIF-1α expression on activation of the PI3K-AKT pathway requires further investigation. In this study, western blotting detected decreased HIF-1α levels when cells were treated with 25 μM LY294002 for 24 h under hypoxia (Fig. 7. A and F). Additionally, the phosphorylation of the PI3K-AKT pathway was reduced when HIF-1α was inhibited by LW6 (Fig. 7. G, I and L). Collectively, these results suggest that PI3K activation in KFb promotes HIF-1α protein levels, and HIF-1α responds in a positive feedback manner.

Discussion

Keloid scarring is a natural human disease model involving chronic inflammation, fibrosis, and tumors, and is characterized by uncontrolled proliferation of fibroblasts and excessive deposition of extracellular matrix [5, 6, 27]. Aerobic glycolysis is considered a hallmark of cancer [28]. Tissue hypoxia is commonly found in most solid tumors and results in metabolic reprogramming. Our previous work demonstrated metabolic reprogramming and the augmented activation of the PI3K/AKT pathway in KFb under hypoxic conditions [15]. However, the role of the PI3K/AKT pathway in modulating glucose metabolism and cell functions in KFb under hypoxia is poorly documented. In the present study, we investigated glycolysis, mitochondrial function, and cell function after PI3K inhibition both under hypoxia and normoxia. In addition, redox homeostasis, along with the relationship between the PI3K-AKT signaling network and HIF-1α were also explored under hypoxia.

The PI3K-AKT signaling network represents the main growth regulatory pathways in mammalian cells, and abnormal activation of this signaling network is considered to be one of the most frequently altered pathways in human cancers [29]. PI3K, which exists as a heterodimer of a catalytic subunit coupled with a regulatory subunit [30], mainly transfers signals from G protein-coupled receptors (GPCRs) and receptor tyrosine kinases (RTKs), thereby regulating physiological functions of cells [22]. Besides directly regulating multiple cellular biological processes, including growth, proliferation, and survival, the PI3K signaling network is implicated in metabolic reprogramming. Extensive studies conducted in recent decades have illustrated that the ubiquitous PI3K-AKT pathway exerts a regulatory role in cellular metabolism by either directly modulating metabolic enzymes and nutrient transporters or by controlling transcription factors that regulate the expression levels of critical components of metabolic pathways [23]. Accumulating evidence reveals that PI3K signaling directly regulates glucose uptake and glycolysis in most human cancers. A recent study demonstrated that the PI3K-AKT-mTOR/PFKFB3 pathway promotes aerobic glycolysis in lung fibroblasts and collagen synthesis in lipopolysaccharide-induced pulmonary fibrosis [31]. Keloids exhibit physiological functions similar to those of tumors and fibrotic diseases. However, the regulation of the PI3K-AKT signaling network in glucose metabolism in KFb under hypoxia remains unclear. In our study, the PI3K blockade decreased the protein expression of GLUT1 and LDHA in KFb, suggesting that the activation of the PI3K-AKT pathway promotes glucose intake and enhances the Warburg effect. Additionally, we also detected decreased levels of glycolytic enzymes, including HK2, PFKFB3, PGK1, ENO1, and PKM2, after PI3K inhibition using LY294002 under hypoxic conditions. ECAR indicates real-time changes in glycolytic levels in living cells. When PI3K signaling was inhibited, the results of the glycolytic stress test showed attenuated ECAR, including basic glycolysis, glycolytic capacity, and glycolytic reserve.

The PI3K-AKT signaling pathway is crucial for maintaining mitochondrial function and healthy conditions. Although the regulation of PI3K-AKT signaling in mitochondrial functions has been extensively studied, conflicting findings have been reported. Studies in the last decade have revealed that the PI3K-AKT pathway is negatively related to mitochondrial respiration. Zheng et al. reported that increased phosphorylation in the PI3K-AKT pathway induced by salidroside-inhibited mitochondrial

respiratory chain complex I, disturbed phosphorylation coupling, and moderately depolarized the mitochondrial membrane potential in hepatocytes [32]. Zhao et al. [33] found that blockade of AKT activation by PTEN overexpression suppressed glucose uptake and lactate production and maintained mitochondrial functions, resulting in the transformation of energetic metabolism from glycolysis to oxidative phosphorylation in cultured PTEN-negative human hepatocellular carcinoma (HHCC) cells. In this study, we detected increased mitochondrial mass and MMP in KFb after PI3K inhibition with LY294002. Consistent with previous studies [32, 33], PI3K inactivation enhanced mitochondrial function in our study. Additionally, we also observed mitochondrial ultrastructure, and TEM analysis revealed that the mitochondrial ultrastructure remained previous conditions when KFb was treated with LY294002. We evaluated OCR, representing mitochondrial respiration, using a Seahorse XFp Real-time Extracellular Flux Analyzer in real time. The results demonstrated that KFb treated with PI3K inhibition exhibited increased OCR parameters, including basal respiration, maximal respiration, spare capacity, and ATP production. Hence, our findings collectively indicate that PI3K inhibition suppresses glycolysis and enhances mitochondrial respiration. However, a growing body of evidence has revealed that activation of PI3K is positively associated with mitochondrial function. Activation of PI3K/AKT signaling with the activator IGF-1 resulted in enhanced glycolysis and upregulation of mitochondrial complex I expression and activity in isogenic hepatocyte cell lines [34]. Li et al. [35] reported that activation of PI3K/AKT due to PTEN loss increases mitochondrial mass and function by regulating estrogen-related receptor α (ERRα) through the AKT/CREB axis in primary hepatocytes.

However, the modulation of the PI3K-AKT pathway in KFb proliferation, migration, invasion, and apoptosis requires further investigation. In this study, KFb was treated with a range of concentrations of LY294002 and incubated under hypoxic or normoxic conditions, following which the functions described above were determined. Interestingly, our findings were consistent with those of previous studies that focused on diverse conditions [36–39]. The results of cell counting showed that PI3K inhibition compromised KFb proliferation in a dose- and time-dependent manner. Furthermore, the inhibition of PI3K on proliferation under hypoxic conditions was more sensitive than that under normoxia. It is generally believed that the PI3K-AKT pathway is closely linked to invasion through the regulation of MMP-2 and MMP-9 expression. The findings of the Transwell chamber suggested that migration and invasion were significantly inhibited in the blockade of the PI3K-AKT signaling pathway. Additionally, the PI3K-AKT signaling network is implicated in mitochondrial apoptosis. We observed that PI3K inhibition markedly promoted KFb apoptosis. Moreover, the pro-apoptotic effect was more distinct under hypoxic conditions. Similar results were observed for keloid fibroblasts. Xin et al. reported that the PI3K/AKT/mTOR pathway activated by CD26 promotes proliferation and invasion in keloid fibroblasts [40]. A recent report by Lv et al. [41] revealed that inactivation of the PI3K/Akt signaling pathway by circCOL5A1 knockdown in the keloid inhibited KFb proliferation, migration, and enhanced apoptosis. Additionally, we investigated whether the PI3K-AKT pathway regulates KFb proliferation through glycolysis. The ECAR decreased or increased when KFb was treated with a PI3K inhibitor or PI3K activator, respectively. Interestingly, the glycolysis stress test suggested that KFb treated with both PI3K activation and glycolysis inhibition manifested significantly lower ECAR parameters than the control group. We concluded that glycolysis is

partly regulated by the PI3K-AKT pathway. It is widely acknowledged that glycolysis and OXPHOS are the two main sources of energy generation. When one pathway is inhibited, cells would tend to depend largely on the other pathway for ATP provision. Hence, KFb exhibited increased OCR when cells were treated with a PI3K inhibitor or PI3K activator coupled with a glycolysis inhibitor. But one point to note is that ATP generation in SC79 and 2-DG group did not increase compared to SC79 group under hypoxia and the special phenomenon needs further study. Furthermore, the proliferative rate of KFb treated with the PI3K activator and glycolysis inhibitor was significantly inhibited compared to that of PI3K activation. These results collectively indicate that the proliferation induced by glycolysis partly depends on the PI3K-AKT pathway. The conclusion that the PI3K-AKT pathway promotes proliferation by enhancing glycolysis is supported by recent studies focusing on tumor metabolism. Hussain et al. reported that inhibition of glycolysis and lipogenesis by the PI3K inhibitor, 3-Dihydro-2-(naphthalene-1-yl) quinazolin-4(1H)-one (DHNQ) represses angiogenesis and decreases proliferation of colon cancer cells [42]. In a recent study by Wang et al., FoxA2 inhibited the proliferation of hepatic progenitor cells by attenuating PI3K-AKT-HK2-mediated glycolysis [43]. Additionally, glycolysis induced by the PI3K-AKT pathway also plays a key role in invasion and apoptosis in other cancer cells, such as breast cancer [44] and pediatric osteosarcoma [45]. Keloid features with tumor-like physiological functions. Accordingly, we postulated that the PI3K-AKT network can also regulate invasion and apoptosis by glycolysis.

The PI3K-AKT signaling network and HIF-1α are considered the two main pathways for glucose metabolic regulation under hypoxia [46]. However, the relationship between these two pathways remains controversial. An increasing number of studies have demonstrated that activation of PI3K signaling facilitates HIF-1α accumulation in mammalian cells under hypoxic conditions [47–49]. However, the role of HIF-1α in regulating phosphorylation of the PI3K-AKT pathway remains largely unexplored. In the present study, we found that HIF-1α levels decreased when the PI3K-AKT signaling pathway was inhibited by LY294002 in KFb under hypoxia. Moreover, the phosphorylation of the PI3K-AKT pathway was reduced when HIF-1α was inhibited by LW6. This suggests that HIF-1α responds to PI3K signaling in a positive feedback manner. Additionally, Sun et al. reported that HIF1α inhibitor YC-1 inhibits activation of the PI3K/AKT/mTOR pathway during hypoxia in prostate cancer cells [50]. These results collectively suggest that the PI3K-AKT pathway interacts with HIF-1α through a positive feedback mechanism under hypoxia.

We are aware that there are several limitations in the present study. Our understanding of the role of the PI3K-AKT pathway in glucose metabolism in vivo is hindered by the absence of a suitable animal model. Furthermore, further investigation is needed to focus on the regulation of the key metabolic modulator HIF-1α in glycolysis and mitochondrial functions under hypoxia.

Conclusions

In summary, our findings demonstrated the critical regulation of the PI3K-AKT signaling network in glucose metabolism and cell functions in KFb under hypoxia (Figure. 8). PI3K inhibition attenuated the protein expression of glycolytic enzymes and key parameters of ECAR. Inactivation of the PI3K-AKT pathway induces a metabolic shift from glycolysis to mitochondrial oxidative phosphorylation.

Additionally, we revealed that the PI3K-AKT pathway maintains redox homeostasis and that a positive feedback mechanism exists between PI3K-AKT signaling and HIF-1α. Our findings enhance the understanding of the PI3K-AKT pathway and glucose metabolism in keloid pathological mechanisms under hypoxia. Targeting PI3K inhibition to alter glucose metabolism appears to be a promising strategy for keloid prevention and treatment.

Abbreviations

BSA: bull serum albumin; DMEM: dulbecco's modified eagle's medium; ECAR: extracellular acidification rate; ECM: extracellular matrix; EMT: epithelial-mesenchymal transition; ERRα: estrogen-related receptor α; FBS: fetal bovine serum; FOXO: forkhead box O; GPCRs: G protein-coupled receptors; GSK3: glycogen synthase kinase 3; HIF-1α: hypoxia inducible factor-1α; HK2: hexokinase 2; KFb: keloid fibroblasts; mitoROS: mitochondrial ROS; MMP: mitochondrial membrane potential; mTORC1: mammalian target of rapamycin complex 1; OCR: oxygen consumption rate; PBS: phosphate-buffered saline; PDK1: pyruvate dehydrogenase kinase 1; PFK1: phosphofructokinase 1; PIP2: phosphatidylinositol- 4:5-bisphosphate; PIP3: phosphatidylinositol- 3:4:5-trisphosphate; PTEN: phosphatase and tensin homolog deleted on chromosome ten; PVDF: polyvinylidene difluoride; ROS: reactive oxygen species; RTK: receptor tyrosine kinases; SDS-PAGE: sodium dodecyl sulfatepolyacrylamide gel electrophoresis; TEM: transmission electron microscope; 2-DG: 2-deoxy-d-glucose.

Declarations

Acknowledgments

We are extremely grateful for the plastic surgeon and the central laboratory platform for the specimens and services, respectively.

Author contributions

Qifei Wang and Xin Yang performed the experiments, analyzed data, prepared figures, and wrote the manuscript; Jianxun Ma and Xiang Xie carried out the Seahorse experiments and analysis; Yimou Sun and Xu Chang participated in experiments; Hongsen Bi collected samples; Hongyu Xue contributed to the study concept and design. Zelian Qin revised the manuscript. All authors read and approved the final manuscript.

Funding

This work was supported by National Natural Science Foundation of China [grant number 81772090].

Availability of data and materials

All the datasets generated during this study and supporting the conclusions of this article are included within the article and its supplementary figures.

Ethics approval and consent to participate

The studies regarding the clinical samples received approval and were carried out in accordance with the approved guidelines from the Peking University Third Hospital Research Ethics Board (IRB00006761 2014173).

Consent for publication

Not applicable.

Competing interests

The authors declare that they have no competing interests.

Author details

Department of Plastic Surgery, Peking University Third Hospital, 49 North Garden Road, Haidian District, Beijing, China

References

1. He Y, Deng Z, Alghamdi M, Lu L, Fear MW, He L. From genetics to epigenetics: new insights into keloid scarring. Cell Prolif. 2017; 50(2).
2. Lv W, Ren Y, Hou K, Hu W, Yi Y, Xiong M, Wu M, Wu Y, Zhang Q. Epigenetic modification mechanisms involved in keloid: current status and prospect. Clin Epigenetics. 2020; 12(1):183.
3. Hu ZC, Shi F, Liu P, Zhang J, Guo D, Cao XL, Chen CF, Qu SQ, Zhu JY, Tang B. TIEG1 Represses Smad7-Mediated Activation of TGF-beta1/Smad Signaling in Keloid Pathogenesis. J Invest Dermatol. 2017; 137(5):1051-1059.
4. Lv W, Ren Y, Hou K, Hu W, Yi Y, Xiong M, Wu M, Wu Y, Zhang Q. Epigenetic modification mechanisms involved in keloid: current status and prospect. Clin Epigenetics. 2020; 12(1):183.
5. Wang Z, Zhao W, Cao Y, Liu Y, Sun Q, Shi P, Cai J, Shen XZ, Tan W. The Roles of Inflammation in Keloid and Hypertrophic Scars. Front Immunol. 2020; 11.
6. Tan S, Khumalo N, Bayat A. Understanding Keloid Pathobiology From a Quasi-Neoplastic Perspective: Less of a Scar and More of a Chronic Inflammatory Disease With Cancer-Like Tendencies. Front Immunol. 2019; 10.
7. Singer K, Kastenberger M, Gottfried E, Hammerschmied CG, Buttner M, Aigner M, Seliger B, Walter B, Schlosser H, Hartmann A, et al. Warburg phenotype in renal cell carcinoma: high expression of glucose-transporter 1 (GLUT-1) correlates with low CD8(+) T-cell infiltration in the tumor. Int J Cancer. 2011; 128(9):2085-95.
8. Glass DN. Current Understanding of the Genetic Causes of Keloid Formation. J Investig Dermatol Symp Proc. 2017; 18(2):S50-S53.

9. Morris O, Deng H, Tam C, Jasper H. Warburg-like Metabolic Reprogramming in Aging Intestinal Stem Cells Contributes to Tissue Hyperplasia. Cell Rep. 2020; 33(8):108423.
10. Yang L, Xie M, Yang M, Yu Y, Zhu S, Hou W, Kang R, Lotze MT, Billiar TR, Wang H, et al. PKM2 regulates the Warburg effect and promotes HMGB1 release in sepsis. Nat Commun. 2014; 5:4436.
11. Atlante A, de Bari L, Bobba A, Amadoro G. A disease with a sweet tooth: exploring the Warburg effect in Alzheimer's disease. Biogerontology. 2017; 18(3):301-319.
12. Okuno R, Ito Y, Eid N, Otsuki Y, Kondo Y, Ueda K. Upregulation of autophagy and glycolysis markers in keloid hypoxic-zone fibroblasts: Morphological characteristics and implications. Histol Histopathol. 2018; 33(10):1075-1087.
13. Kim J, Kim B, Kim SM, Yang CE, Song SY, Lee WJ, Lee JH. Hypoxia-Induced Epithelial-To-Mesenchymal Transition Mediates Fibroblast Abnormalities via ERK Activation in Cutaneous Wound Healing. Int J Mol Sci. 2019; 20(10).
14. Lei R, Li J, Liu F, Li W, Zhang S, Wang Y, Chu X, Xu J. HIF-1alpha promotes the keloid development through the activation of TGF-beta/Smad and TLR4/MyD88/NF-kappaB pathways. Cell Cycle. 2019; 18(23):3239-3250.
15. Wang Q, Wang P, Qin Z, Yang X, Pan B, Nie F, Bi H. Altered glucose metabolism and cell function in keloid fibroblasts under hypoxia. Redox Biol. 2021; 38:101815.
16. Kang Y, Roh MR, Rajadurai S, Rajadurai A, Kumar R, Njauw CN, Zheng Z, Tsao H. Hypoxia and HIF-1alpha Regulate Collagen Production in Keloids. J Invest Dermatol. 2020; 140(11):2157-2165.
17. Xie Y, Shi X, Sheng K, Han G, Li W, Zhao Q, Jiang B, Feng J, Li J, Gu Y. PI3K/Akt signaling transduction pathway, erythropoiesis and glycolysis in hypoxia (Review). Mol Med Rep. 2019; 19(2):783-791.
18. Janku F, Yap TA, Meric-Bernstam F. Targeting the PI3K pathway in cancer: are we making headway? Nat Rev Clin Oncol. 2018; 15(5):273-291.
19. Lien EC, Dibble CC, Toker A. PI3K signaling in cancer: beyond AKT. Curr Opin Cell Biol. 2017; 45:62-71.
20. Chen T, Zhang Y, Liu Y, Zhu D, Yu J, Li G, Sun Z, Wang W, Jiang H, Hong Z. MiR-27a promotes insulin resistance and mediates glucose metabolism by targeting PPAR-gamma-mediated PI3K/AKT signaling. Aging (Albany NY). 2019; 11(18):7510-7524.
21. Gao T, Zhang X, Zhao J, Zhou F, Wang Y, Zhao Z, Xing J, Chen B, Li J, Liu S. SIK2 promotes reprogramming of glucose metabolism through PI3K/AKT/HIF-1alpha pathway and Drp1-mediated mitochondrial fission in ovarian cancer. Cancer Lett. 2020; 469:89-101.
22. Fruman DA, Chiu H, Hopkins BD, Bagrodia S, Cantley LC, Abraham RT. The PI3K Pathway in Human Disease. Cell. 2017; 170(4):605-635.
23. Hoxhaj G, Manning BD. The PI3K-AKT network at the interface of oncogenic signalling and cancer metabolism. Nat Rev Cancer. 2020; 20(2):74-88.
24. Semenza GL. Targeting HIF-1 for cancer therapy. Nat Rev Cancer. 2003; 3(10):721-732.

25. Duevel K, Yecies JL, Menon S, Raman P, Lipovsky AI, Souza AL, Triantafellow E, Ma Q, Gorski R, Cleaver S, et al. Activation of a Metabolic Gene Regulatory Network Downstream of mTOR Complex 1. Mol Cell. 2010; 39(2):171-183.
26. Van Dang C. Myc, metabolism, and cancer. Clin Cancer Res. 2016; 222.
27. Lee S, Kim SK, Park H, Lee YJ, Park SH, Lee KJ, Lee DG, Kang H, Kim JE. Contribution of Autophagy-Notch1-Mediated NLRP3 Inflammasome Activation to Chronic Inflammation and Fibrosis in Keloid Fibroblasts. Int J Mol Sci. 2020; 21(21).
28. Park JH, Pyun WY, Park HW. Cancer Metabolism: Phenotype, Signaling and Therapeutic Targets. Cells-Basel. 2020; 9(10).
29. Janku F, Yap TA, Meric-Bernstam F. Targeting the PI3K pathway in cancer: are we making headway? Nat Rev Clin Oncol. 2018; 15(5):273-291.
30. Zhang Y, Ng PK, Kucherlapati M, Chen F, Liu Y, Tsang YH, de Velasco G, Jeong KJ, Akbani R, Hadjipanayis A, et al. A Pan-Cancer Proteogenomic Atlas of PI3K/AKT/mTOR Pathway Alterations. Cancer Cell. 2017; 31(6):820-+.
31. Hu X, Xu Q, Wan H, Hu Y, Xing S, Yang H, Gao Y, He Z. PI3K-Akt-mTOR/PFKFB3 pathway mediated lung fibroblast aerobic glycolysis and collagen synthesis in lipopolysaccharide-induced pulmonary fibrosis. Lab Invest. 2020; 100(6):801-811.
32. Zheng T, Yang X, Wu D, Xing S, Bian F, Li W, Chi J, Bai X, Wu G, Chen X, et al. Salidroside ameliorates insulin resistance through activation of a mitochondria-associated AMPK/PI3K/Akt/GSK3beta pathway. Br J Pharmacol. 2015; 172(13):3284-301.
33. Zhao C, Wang B, Liu E, Zhang Z. Loss of PTEN expression is associated with PI3K pathway-dependent metabolic reprogramming in hepatocellular carcinoma. Cell Commun Signal. 2020; 18(1).
34. Li C, Li Y, He L, Agarwal AR, Zeng N, Cadenas E, Stiles BL. PI3K/AKT signaling regulates bioenergetics in immortalized hepatocytes. Free Radical Bio Med. 2013; 60:29-40.
35. Li Y, He L, Zeng N, Sahu D, Cadenas E, Shearn C, Li W, Stiles BL. Phosphatase and Tensin Homolog Deleted on Chromosome 10 (PTEN) Signaling Regulates Mitochondrial Biogenesis and Respiration via Estrogen-related Receptor alpha (ERR alpha). J Biol Chem. 2013; 288(35):25007-25024.
36. Lee J, Liu R, Li J, Wang Y, Tan L, Li X, Qian X, Zhang C, Xia Y, Xu D, et al. EGFR-Phosphorylated Platelet Isoform of Phosphofructokinase 1 Promotes PI3K Activation. Mol Cell. 2018; 70(2):197-+.
37. Huang W, Ding X, Ye H, Wang J, Shao J, Huang T. Hypoxia enhances the migration and invasion of human glioblastoma U87 cells through PI3K/Akt/mTOR/HIF-1alpha pathway. Neuroreport. 2018; 29(18):1578-1585.
38. Liu W, Jing ZT, Xue CR, Wu SX, Chen WN, Lin XJ, Lin X. PI3K/AKT inhibitors aggravate death receptor-mediated hepatocyte apoptosis and liver injury. Toxicol Appl Pharmacol. 2019; 381:114729.
39. Zhou J, Jiang Y, Chen H, Wu Y, Zhang L. Tanshinone I attenuates the malignant biological properties of ovarian cancer by inducing apoptosis and autophagy via the inactivation of PI3K/AKT/mTOR pathway. Cell Proliferat. 2020; 53(2).

40. Xin Y, Min P, Xu H, Zhang Z, Zhang Y, Zhang Y. CD26 upregulates proliferation and invasion in keloid fibroblasts through an IGF-1-induced PI3K/AKT/mTOR pathway. Burns Trauma. 2020; 8:tkaa025.
41. Lv W, Liu S, Zhang Q, Hu W, Wu Y, Ren Y. Circular RNA CircCOL5A1 Sponges the MiR-7-5p/Epac1 Axis to Promote the Progression of Keloids Through Regulating PI3K/Akt Signaling Pathway. Front Cell Dev Biol. 2021; 9:626027.
42. Hussain A, Qazi AK, Mupparapu N, Guru SK, Kumar A, Sharma PR, Singh SK, Singh P, Dar MJ, Bharate SB, et al. Modulation of glycolysis and lipogenesis by novel PI3K selective molecule represses tumor angiogenesis and decreases colorectal cancer growth. Cancer Lett. 2016; 374(2):250-60.
43. Wang P, Cong M, Liu T, Li Y, Liu L, Sun S, Sun L, Zhu Z, Ma H, You H, et al. FoxA2 inhibits the proliferation of hepatic progenitor cells by reducing PI3K/Akt/HK2-mediated glycolysis. J Cell Physiol. 2020; 235(12):9524-9537.
44. Zhang T, Zhu X, Wu H, Jiang K, Zhao G, Shaukat A, Deng G, Qiu C. Targeting the ROS/PI3K/AKT/HIF-1alpha/HK2 axis of breast cancer cells: Combined administration of Polydatin and 2-Deoxy-d-glucose. J Cell Mol Med. 2019; 23(5):3711-3723.
45. Zhuo B, Li Y, Li Z, Qin H, Sun Q, Zhang F, Shen Y, Shi Y, Wang R. PI3K/Akt signaling mediated Hexokinase-2 expression inhibits cell apoptosis and promotes tumor growth in pediatric osteosarcoma. Biochem Biophys Res Commun. 2015; 464(2):401-6.
46. Courtnay R, Ngo DC, Malik N, Ververis K, Tortorella SM, Karagiannis TC. Cancer metabolism and the Warburg effect: the role of HIF-1 and PI3K. Mol Biol Rep. 2015; 42(4):841-51.
47. Wan X, Liu Y, Zhao Y, Sun X, Fan D, Guo L. Orexin A affects HepG2 human hepatocellular carcinoma cells glucose metabolism via HIF-1alpha-dependent and -independent mechanism. Plos One. 2017; 12(9):e0184213.
48. Yang C, Liu X, Zhao K, Zhu Y, Hu B, Zhou Y, Wang M, Wu Y, Zhang C, Xu J, et al. miRNA-21 promotes osteogenesis via the PTEN/PI3K/Akt/HIF-1alpha pathway and enhances bone regeneration in critical size defects. Stem Cell Res Ther. 2019; 10(1):65.
49. Zheng H, Zhou C, Lu X, Liu Q, Liu M, Chen G, Chen W, Wang S, Qiu Y. DJ-1 promotes survival of human colon cancer cells under hypoxia by modulating HIF-1alpha expression through the PI3K-AKT pathway. Cancer Manag Res. 2018; 10:4615-4629.
50. Sun H, Liu Y, Huang Y, Pan S, Huang D, Guh J, Lee F, Kuo S, Teng C. YC-1 inhibits HIF-1 expression in prostate cancer cells: contribution of Akt/NF-kappa B signaling to HIF-1 alpha accumulation during hypoxia. Oncogene. 2007; 26(27):3941-3951.

Figures

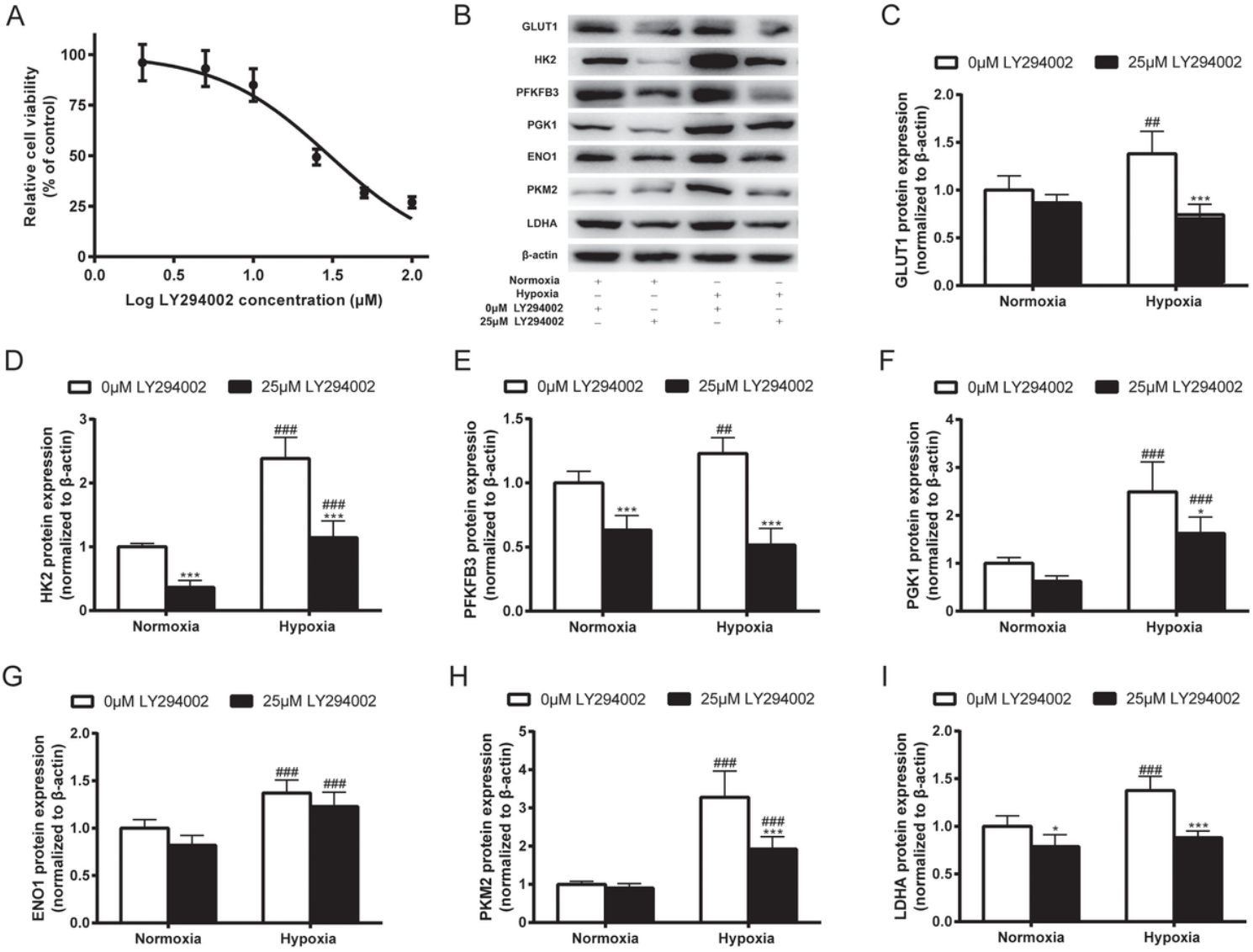

Figure 1

Attenuated glycolysis after inhibition of the PI3K-AKT pathway in KFb. (A) Determination of concentrations of PI3K inhibitors LY294002. KFb were intervened with a series of LY294002 concentrations (0, 1, 5, 10, 25 and 50 μM) under hypoxia for 48h. Cell viabilities were evaluated by cell counting under microscope. (B-I) The protein levels of glycolytic enzymes including GLUT1, HK2, PFKFB3, PGK1, ENO1, PKM2 and LDHA were determined by western blotting. Proteins were collected after KFb were intervened with LY294002 (0 and 25μM) and incubated for 24 h under hypoxia (3%) or normoxia. n=6, *P<0.05, ***P<0.001 compared with the control group under the same oxygen condition. ##P<0.01, ###P<0.001 compared with the normoxicgroup at the same LY294002 concentration.

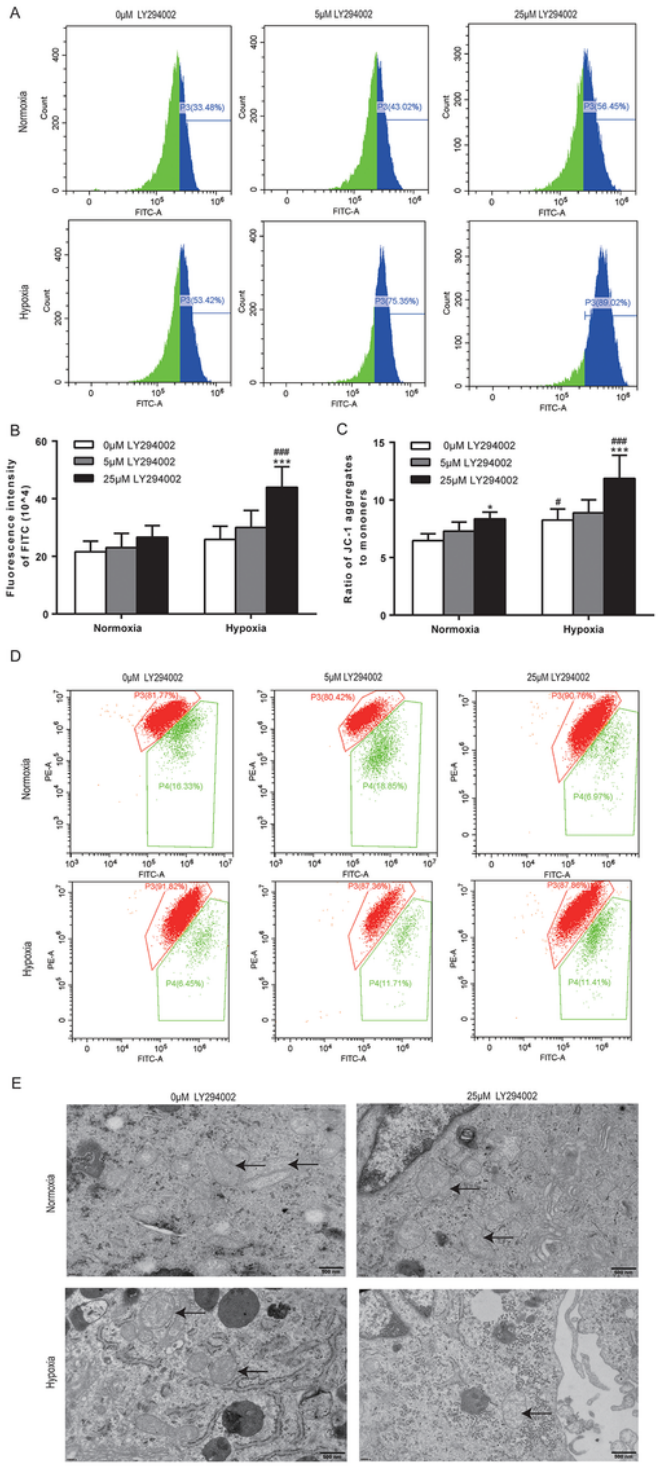

Figure 2

Evaluations of mitochondrial mass, MMP and mitochondrial ultrastructure in KFb after PI3K inhibition. (A-B) Inactivation of PI3K-AKT pathway increased mitochondrial numbers after incubation under hypoxia or normoxia for 48 h, detected by flow cytometry with mitochondrial green explorer. (C-D) PI3K inhibition elevated MMP after cells were cultured under hypoxia or normoxia for 24h, explored by flow cytometry with JC-1. (E) Mitochondrial ultrastructure was observed under ETM. KFb were treated with LY294002 (0

and 25 μM) and incubated for 48 h under hypoxia (3%) or normoxia. The arrow shows the mitochondria. n=6, ***P<0.001 compared with the control group under the same oxygen condition. ###P<0.001 compared with the normoxicgroup at the same LY294002 concentration.

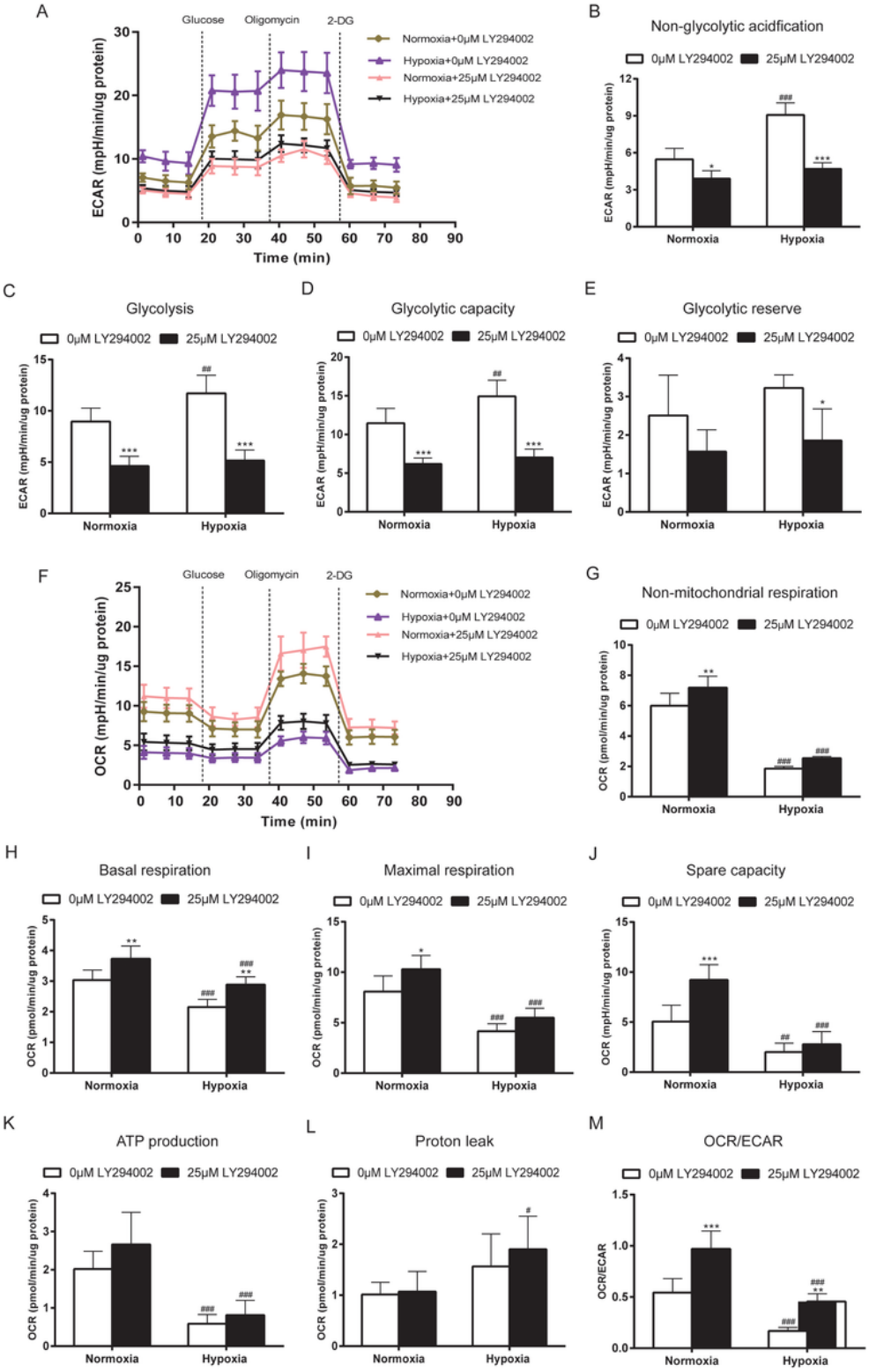

Figure 3

Altered ECAR and OCR after PI3K inactivation in KFb. Representative graphs ofglycolytic stress tests of KFb under normoxia and hypoxia using a Seahorse XF96 Extracellular Flux Analyzer (A). KFb treated with

25 μM LY294002 showed decreased non-glycolytic acidification (B), glycolysis (C), glycolytic capacity (D) and glycolytic reserve (E). Representative graphs of mitochondrial stress tests of KFb (F). PI3K inhibition enhanced non-mitochondrial oxygen consumption (G), basal respiration (H), maximal respiration (I), spare respiratory capacity (J), ATP production (K), proton leak (L) and OCR/ECAR (M). n=6, *P<0.05, **P<0.01, ***P<0.001 compared with the control group under the same oxygen condition. #P<0.05, ##P<0.01, ###P<0.001 compared with the normoxic group at the same LY294002 concentration.

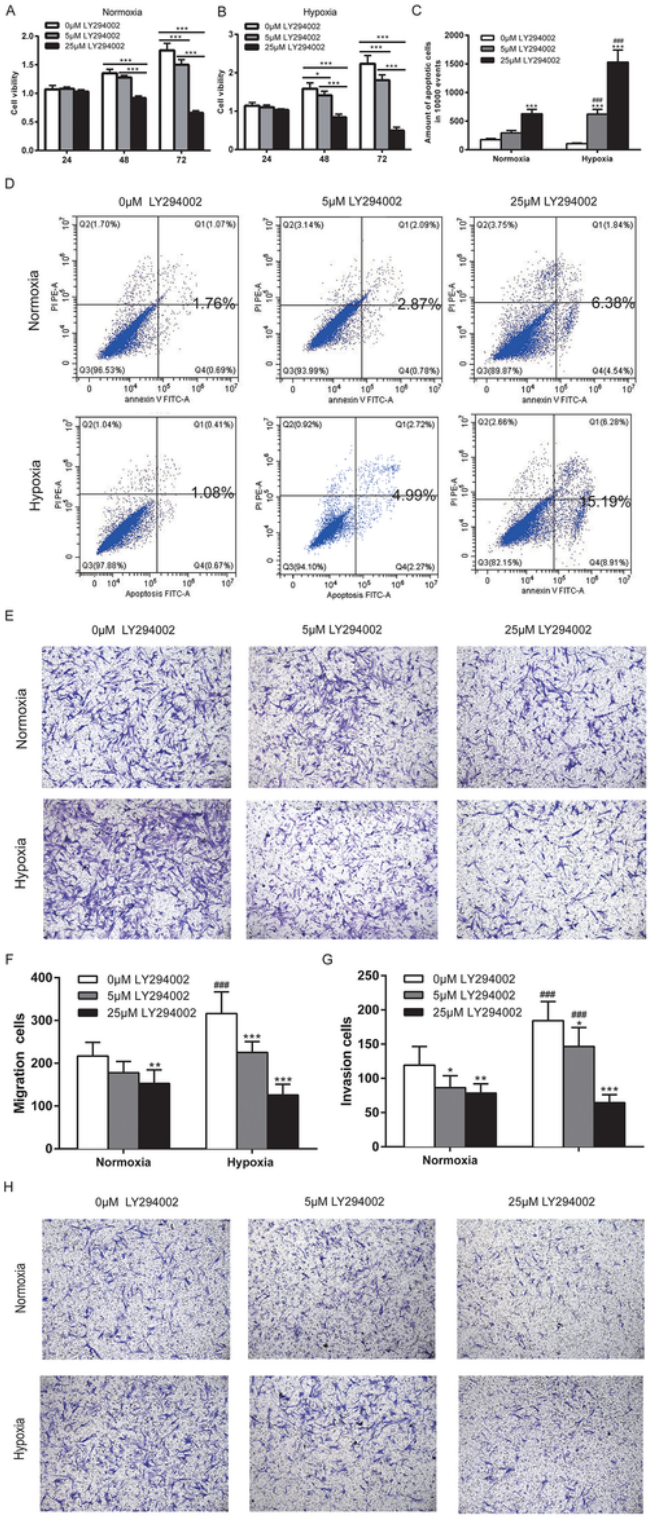

Figure 4

Cell function changes ofKFb after PI3K-AKT pathway was blocked. (A-B) Cell proliferation of KFb were markedly inhibited after treated with LY294002 (0, 5 and 25 μM) under normoxia or hypoxia for 24, 48, 72 h. Cell numbers were determined with cell counting under a microscope. *P<0.05, ***P<0.001 (C-D) Apoptosis was significantly enhanced by PI3K inhibitor. KFb were treated with LY294002 (0, 5 and 25 μM) under normoxia or hypoxia for 48 h, and then apoptotic levels were measured by flow cytometry. Migration (E-F) and invasion (G-H) were attenuated after PI3K inhibition. KFb were treated with LY294002 (0, 5 and 25 μM) for 24 h, and migration and invasion were evaluated with transwell chamber. n=6, *P<0.05, **P<0.01, ***P<0.001 compared with the control group under the same oxygen condition. ###P<0.001 compared with the normoxic group at the same LY294002 concentration.

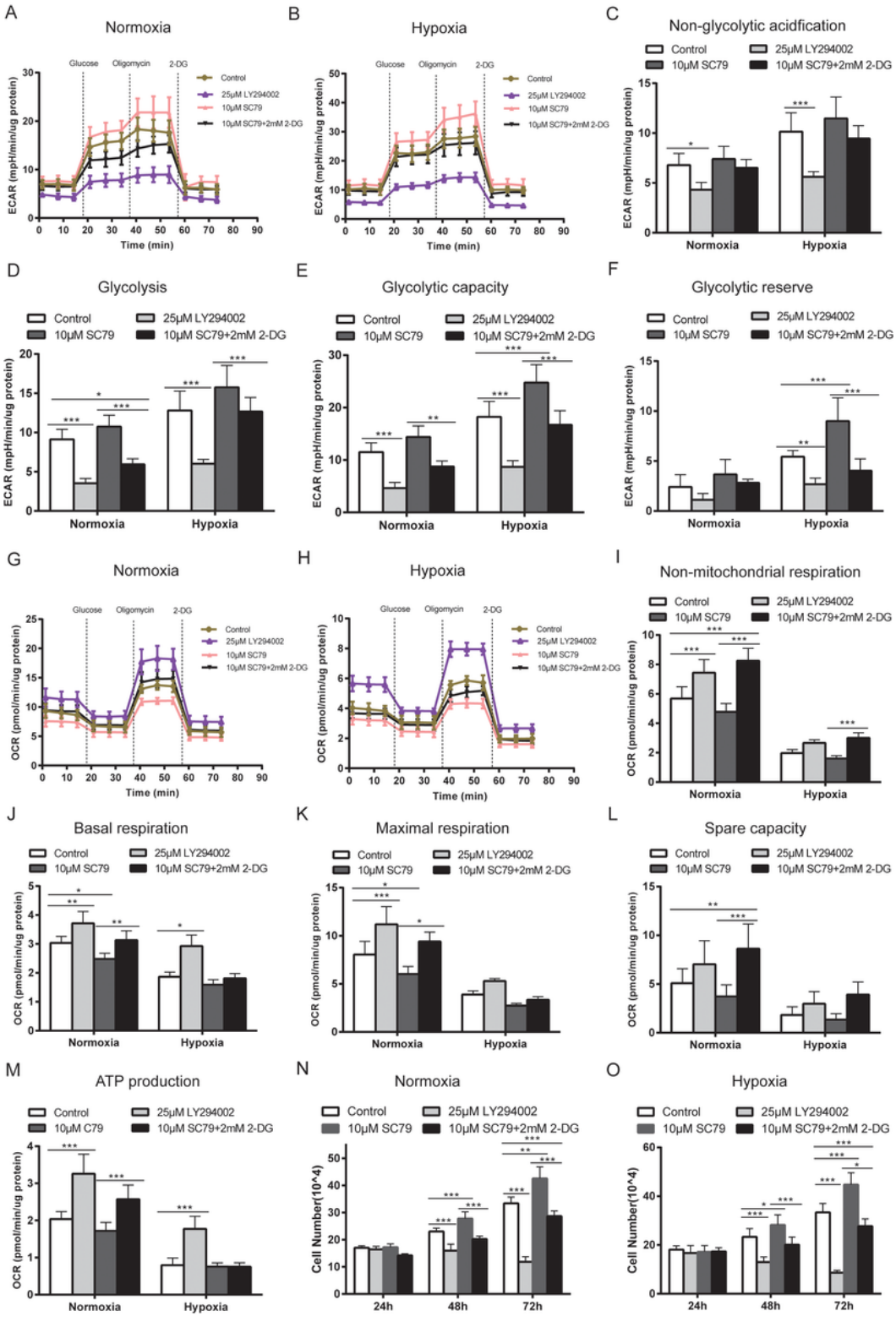

Figure 5

The PI3K-AKT pathway promoted proliferation through regulating glycolysis. (A-B) The promotion of PI3K-AKT pathway on glycolysis was impaired by glycolytic inhibitor 2-DG. Glycolysis key parameters including non-glycolytic acidification (C), glycolysis (D), glycolytic capacity (E) and glycolytic reserve (F) were compromised when KFb were treated glycolysis inhibitor 2-DG combined with PI3K activator SC79 compared with those of only SC79 group. (G-M) Mitochondrial respiration compensatorily increased

when glycolysis enhanced by activated PI3K-AKT pathway was impaired by 2-DG. (N-O) glycolysis was involved in enhanced proliferation by PI3K-AKT pathway. KFb were intervened with PBS, LY294002, SC79, and SC79 combined with 2-DG and cultured under normoxia or hypoxia for 24, 48 and 72 h. n=6, *P<0.05, **P<0.01, ***P<0.001.

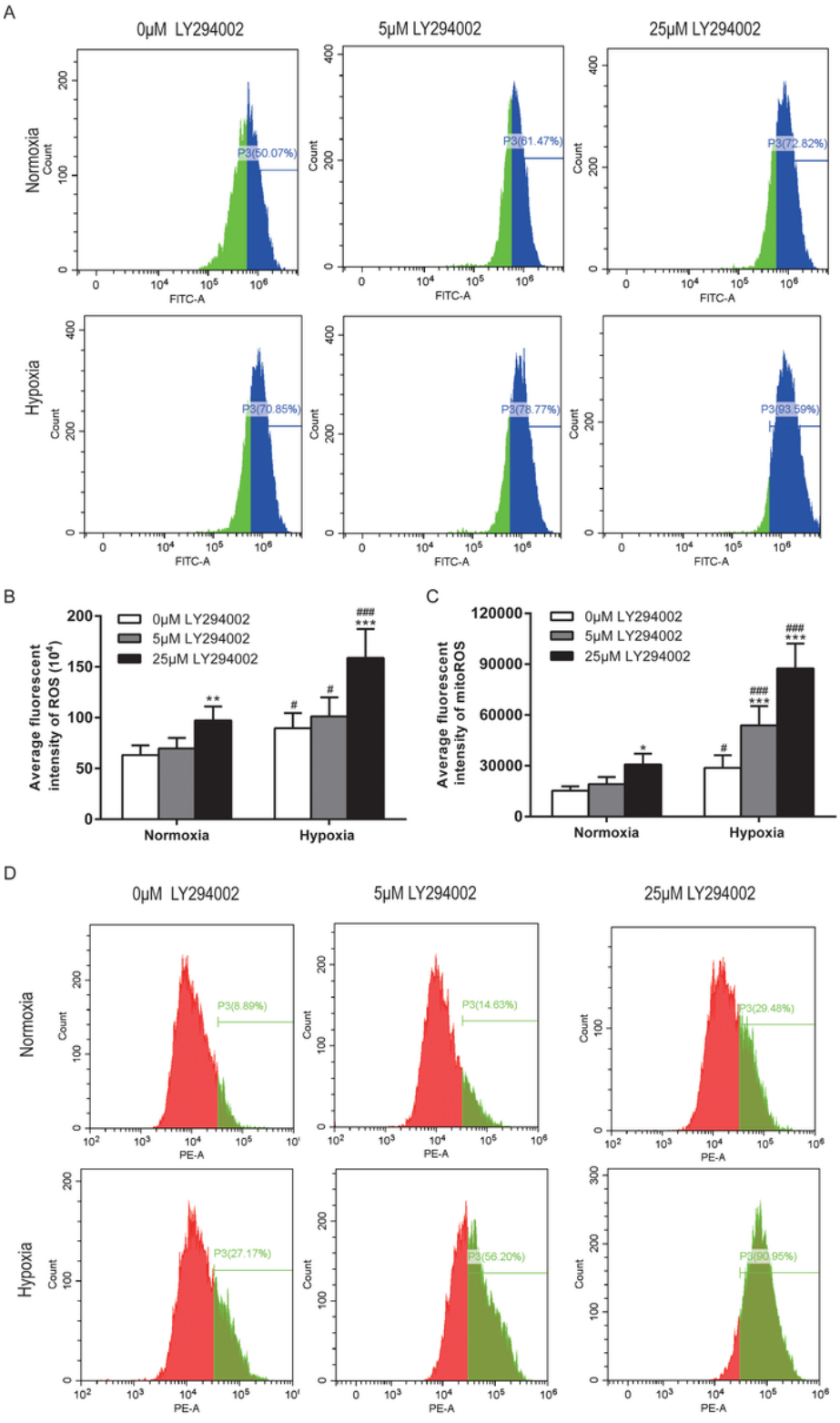

Figure 6

Inhibition of the PI3K-AKT pathway induced ROS generation. After KFb were treated with LY294002 (0, 5 and 25 μM) under normoxia or hypoxia for 24 h, ROS and mitoROS were determined by flow cytometry. PI3K inhibition increased ROS (A-B) and mitoROS (C-D) generation. n=6, *P<0.05, **P<0.01, ***P<0.001 compared with the control group under the same oxygen condition. #P<0.05, ###P<0.001 compared with the normoxiagroup at the same LY294002 concentration.

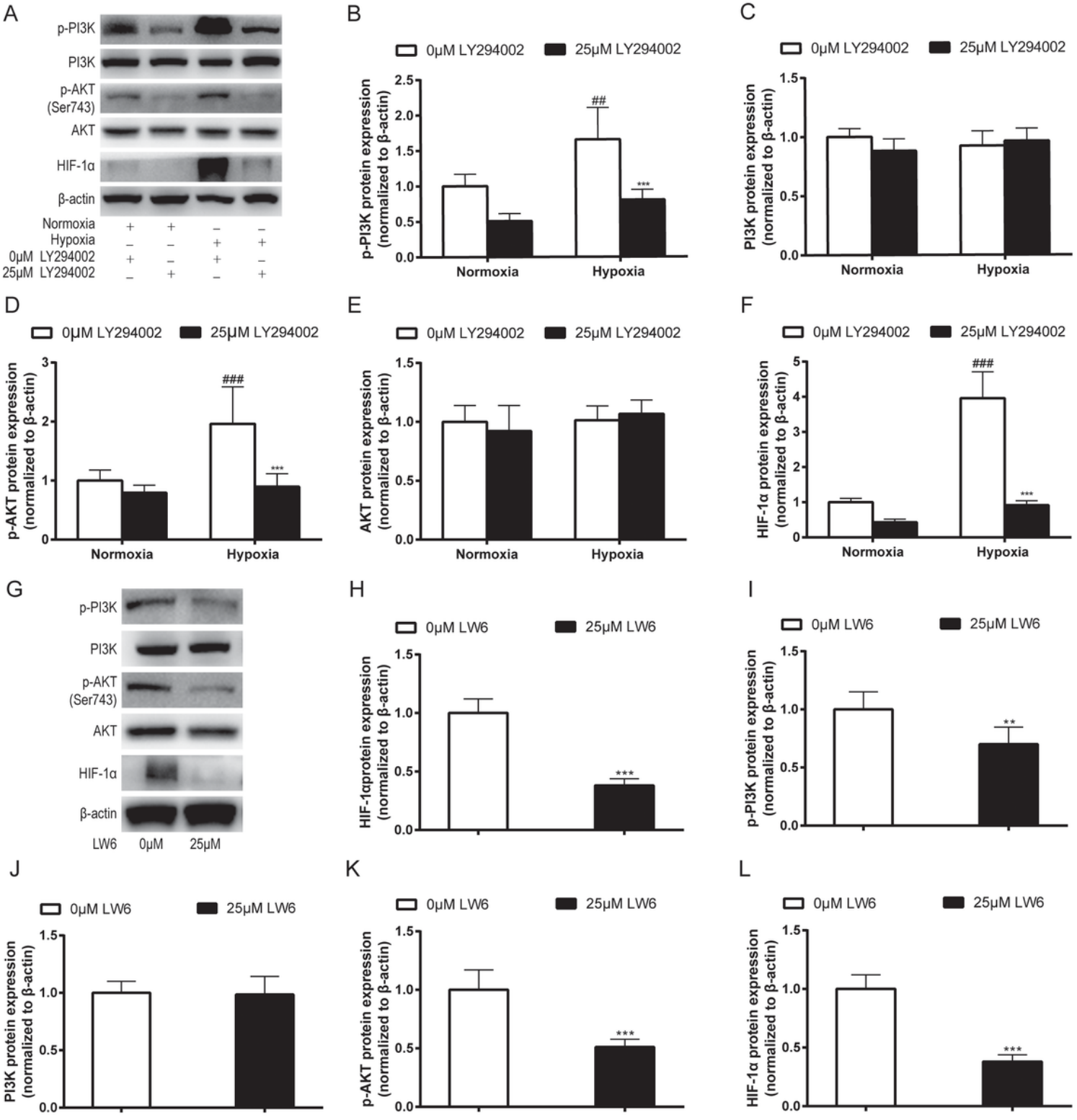

Figure 7

A positive feedback mechanism existed betweenthe PI3K-AKT and HIF1α pathways. KFb were treated with LY294002 (0 and 25 μM) under normoxia or hypoxia for 24 h, and western blot was performed to detected HIF1α protein expression, phosphorylation of PI3K and AKT. (A-F) The HIF1α protein level lowered when PI3K-AKT pathway was blocked. (G-L) Phosphorylation of PI3K-AKT pathway was attenuated when KFb were treated with HIF1α inhibitor LW6 under hypoxia for 24 h. n=6, **P<0.01, ***P<0.001 compared with the control group under the same oxygen condition. ##P<0.01, ###P<0.001 compared with the normoxia group at the same LY294002 concentration.

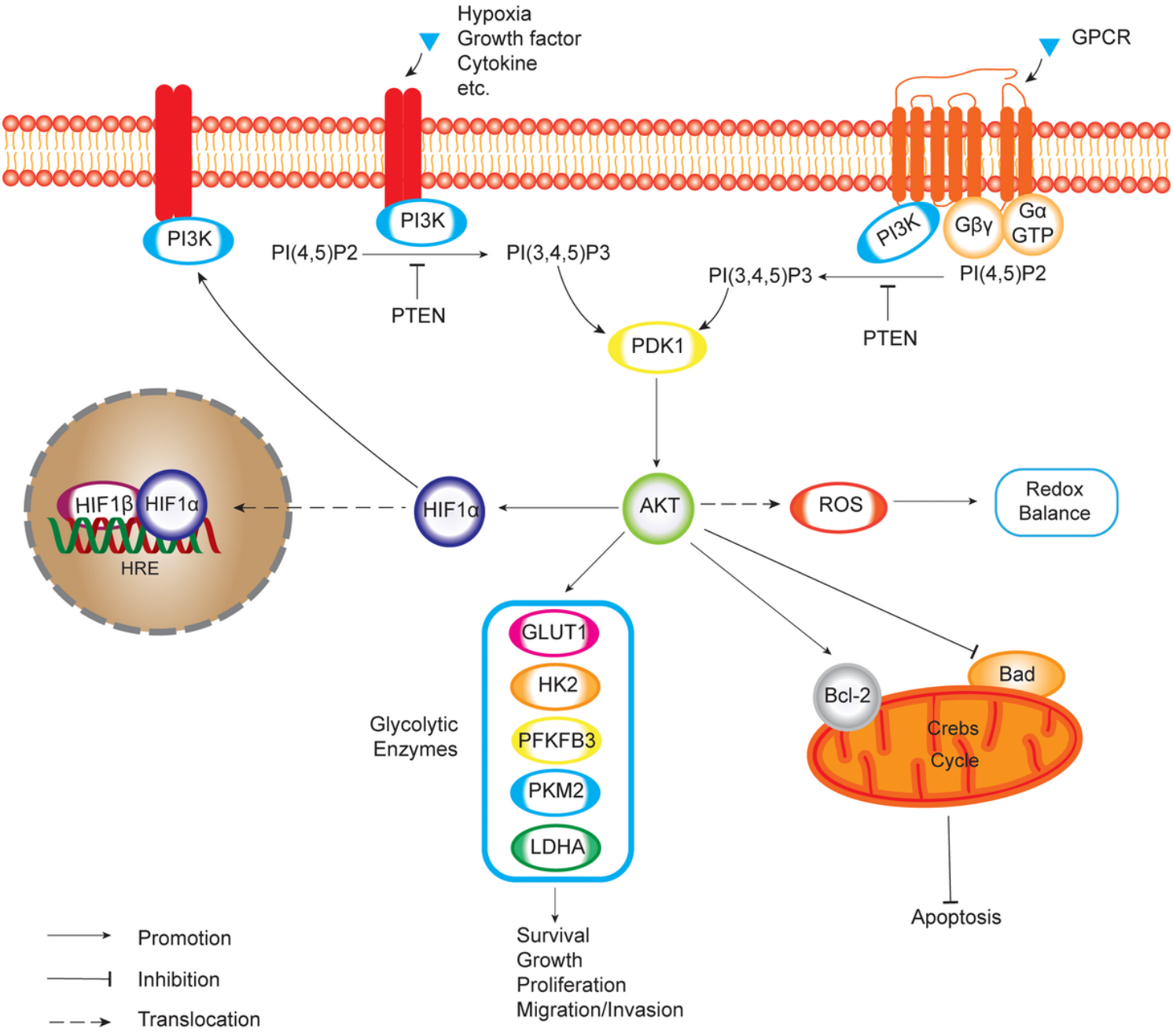

Figure 8

Schematic diagram of regulation of PI3K-AKT pathway on glucose metabolism and cell functions in KFb. PI3K activation induced by growth factor, cytokine, hormone and intergrin etc leads to AKT

phosphorylation through PDK1 activation. AKT activation regulates glucose metabolism including glycolysis and mitochondrial oxidative phosphorylation, resulting in cell survival, growth, proliferation, invasion and apoptosis inhibition.

Supplementary Files

This is a list of supplementary files associated with this preprint. Click to download.

- Supplementarydata.docx